THE JOURNAL OF BIOLOGICAL CHEMISTRY
Vol. 279, No. 5, Issue of January 30, pp. 3612–3619, 2004

Printed in U.S.A.

Interactions of a Family 18 Chitinase with the Designed Inhibitor HM508 and Its Degradation Product, Chitobiono-δ-lactone*

Received for publication, September 10, 2003, and in revised form, November 3, 2003
Published, JBC Papers in Press, November 3, 2003, DOI 10.1074/jbc.M310057200

Gustav Vaaje-Kolstad‡, Andrea Vasella§, Martin G. Peter¶, Catharina Netter‖, Douglas R. Houston‖, Bjørge Westereng‡, Bjørnar Synstad‡, Vincent G. H. Eijsink‡, and Daan M. F. van Aalten‖‡‡**

From the ‡Department of Chemistry and Biotechnology, Agricultural University of Norway, N-1432 Ås, Norway, the §Eidgenössische Technische Hochschule Hönggerberg, CH-8093 Zürich, Switzerland, the ¶Institute of Chemistry, University of Potsdam, D-14469 Potsdam, Germany, and the ‖Division of Biological Chemistry and Molecular Microbiology, School of Life Sciences, University of Dundee, Dundee DD1 5EH, Scotland

We describe enzymological and structural analyses of the interaction between the family 18 chitinase ChiB from *Serratia marcescens* and the designed inhibitor *N*,*N*′-diacetylchitobionoxime-*N*-phenylcarbamate (HM508). HM508 acts as a competitive inhibitor of this enzyme with a K_i in the 50 μM range. Active site mutants of ChiB show K_i values ranging from 1 to 200 μM, providing insight into some of the interactions that determine inhibitor affinity. Interestingly, the wild type enzyme slowly degrades HM508, but the inhibitor is essentially stable in the presence of the moderately active D142N mutant of ChiB. The crystal structure of the D142N-HM508 complex revealed that the two sugar moieties bind to the −2 and −1 subsites, whereas the phenyl group interacts with aromatic side chains that line the +1 and +2 subsites. Enzymatic degradation of HM508, as well as a Trp → Ala mutation in the +2 subsite of ChiB, led to reduced affinity for the inhibitor, showing that interactions between the phenyl group and the enzyme contribute to binding. Interestingly, a complex of enzymatically degraded HM508 with the wild type enzyme showed a chitobiono-δ-lactone bound in the −2 and −1 subsites, despite the fact that the equilibrium between the lactone and the hydroxy acid forms in solution lies far toward the latter. This shows that the active site preferentially binds the ^4E conformation of the −1 sugar, which resembles the proposed transition state of the reaction.

Chitin, a structural component of invertebrate exoskeletons and fungal cell walls, is an abundant, rigid, linear carbohydrate polymer consisting of β(1, 4)-linked *N*-acetyl-glucosamine (GlcNAc) units. In nature, chitin is degraded by chitinases and β-*N*-acetylhexosaminidases belonging to families 18 and 19 and families 3 and 20 of glycoside hydrolase, respectively (1–3). Chitinases occur in a variety of organisms from bacteria and fungi to plants and vertebrates. It has been shown that inhibitors of family 18 chitinases affect the life cycles of insects (4–6) and human pathogens such as *Candida albicans* (7) and the human malaria parasite *Plasmodium falciparum* (8–10). Thus, family 18 chitinases have been proposed as targets for the development of drugs and insecticides.

Structural and enzymological studies of several family 18 chitinases have provided detailed insight into the catalytic center and mechanism of these enzymes (11–15). Leaving group departure is promoted by a glutamate residue that acts as catalytic acid (Glu-144 in chitinase B (ChiB)[1] from *Serratia marcescens*, the enzyme used in this study). The emerging positive charge on the anomeric carbon is stabilized by concomitant nucleophilic attack of the *N*-acetyl group of the −1 sugar on the anomeric carbon, which leads to formation of an oxazolinium ion intermediate (Fig. 1). Glu-144 is located near the end of β-strand 4 of the catalytic $(\beta\alpha)_8$ barrel and is preceded by other conserved acidic residues that are located in the core and are essential for catalysis (Asp-140 and Asp-142 in ChiB) (13–17). Asp-142 contributes to the correct positioning of the *N*-acetyl group of the −1 sugar, modulation of the pK_a of Glu-144 during the catalytic cycle, and stabilization of the oxazolinium ion intermediate. Mutation of Asp-142 to Ala in ChiB almost completely abolishes catalytic activity, whereas mutation to Asn reduces activity ~50-fold (13, 17).

The best known inhibitor of family 18 chitinases is allosamidin (18) (Fig. 1), a pseudotrisaccharide that inhibits with K_i values in the 1 nM–1 μM range (19). Structural studies have shown that allosamidin binds in the −3 to −1 subsites (13, 15, 20–22). The moiety bound to the −1 subsite is an allosamizoline, which resembles the oxazolinium ion reaction intermediate (Fig. 1). The only other known high affinity inhibitors of family 18 chitinases are the naturally occurring cyclopentapeptides argadin (4) and argifin (23). Structural and enzymological analyses have shown that these peptides bind intimately to the active site of ChiB with affinities in the 10 nM (argadin) and 10 μM (argifin) range (24).

Although total syntheses of allosamidin have been reported (reviewed in Ref. 25), these syntheses are lengthy and do not offer a practical access to the inhibitor. Until recently, allosamidin was commercially available at a cost of $500 (United States currency) per milligram, but it is currently not being sold. No total synthesis of the cyclic pentapeptides argifin and argadin has been reported. Attempts to synthesize oligo-Glc-

* This work was supported by the Norwegian Research Council Grants 140497/420 and 140440/130. The costs of publication of this article were defrayed in part by the payment of page charges. This article must therefore be hereby marked "*advertisement*" in accordance with 18 U.S.C. Section 1734 solely to indicate this fact.

The atomic coordinates and structure factors (codes 1UR8 and 1UR9) have been deposited in the Protein Data Bank, Research Collaboratory for Structural Bioinformatics, Rutgers University, New Brunswick, NJ (http://www.rcsb.org/).

** Supported by a Biotechnology and Biological Sciences Research Council (BBSRC) Cooperative Awards in Science and Engineering (CASE) studentship (partner, Cyclacel).

‡‡ Supported by a Wellcome Trust Research Career Development Fellowship, and to whom correspondence should be addressed. Fax: 44-1382-345764; E-mail: dava@davapc1.bioch.dundee.ac.uk.

[1] The abbreviations used are: ChiB, chitinase B; WT, wild type ChiB; HM508, *N*,*N*′-diacetyl-chitobionoxime-*N*-phenylcarbamate; ESI-MS, electrospray ionization mass spectroscopy; BSA, bovine serum albumin.

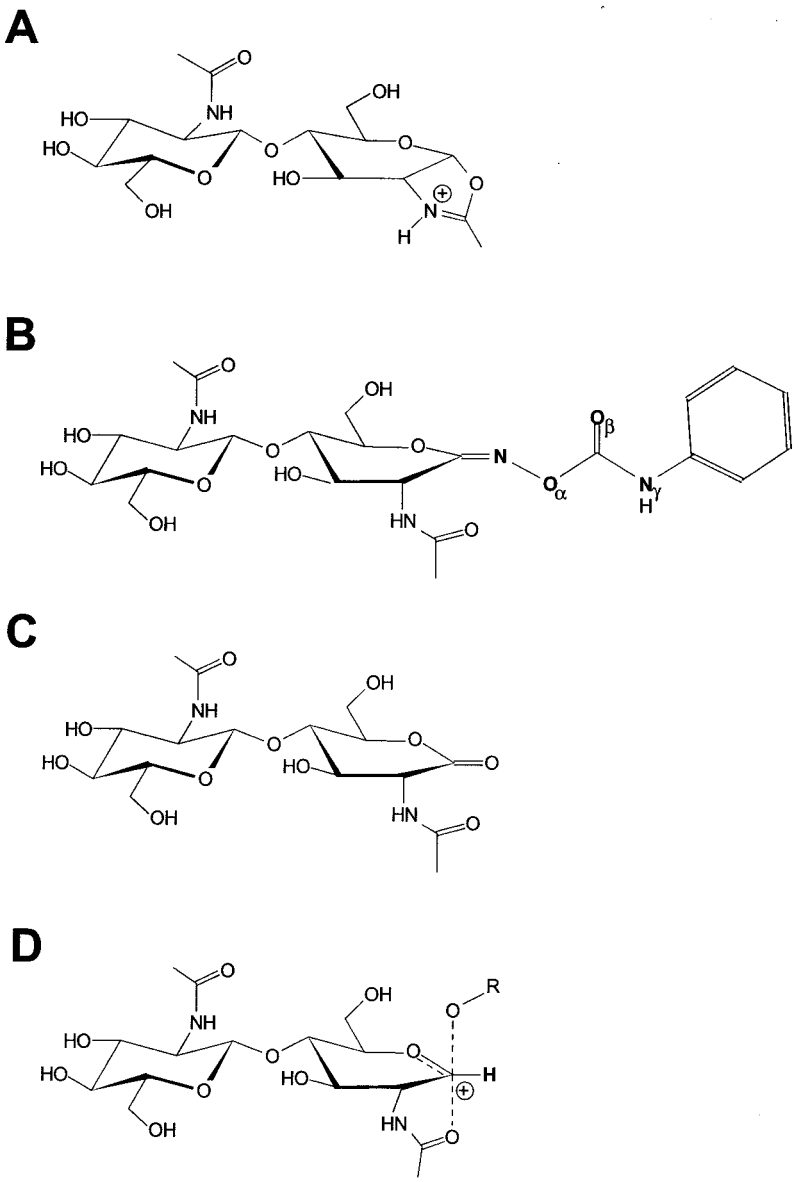

FIG. 1. **Chemical structure of relevant compounds.** *A*, oxazolinium ion reaction intermediate. *B*, HM508 (*N*,*N*′-diacetyl-chitobionoxime-*N*-phenylcarbamate) (M_r = 556). *C*, chitobionolactone (M_r = 421). *D*, the putative structure of the transition state (11–13, 40).

NAc-based chitinase inhibitors have had limited success to date, mainly due to the fact that the affinity of chitinases for short, non-hydrolyzable chitooligosaccharides (*e.g.* $GlcNAc_2$) is usually low and that longer oligosaccharides with higher affinities are too readily degraded. Thus, effective sugar-based inhibitors need to be based on the introduction of non-hydrolyzable bonds between the sugar moieties and/or on combining short chito-oligosaccharides with other structural elements that increase affinity while preventing degradation of the inhibitor. To the best of our knowledge, such designed inhibitors of family 18 chitinases with an affinity in the μM range have not yet been identified.

Here, we study the interaction between the family 18 chitinase ChiB from *S. marcescens* and the previously designed and synthesized $GlcNAc_2$-derivative *N*,*N*′-diacetyl-chitobionoxime-*N*-phenylcarbamate (HM508; Fig. 1) (26). We show that HM508 inhibits ChiB with a K_i in the 50 μM range. The crystal structures of complexes between HM508 and ChiB and ChiB-D142N reveal details of the interactions between the inhibitor and the enzyme. The importance of some of these interactions was probed by studying the effects of two site-directed mutations (M212A, W220A) in the active site of ChiB on the affinity for HM508. We also show that ChiB is capable of slowly hydrolyzing HM508 to chitobionolactone/chitobiono-hydroxy acid and that the enzyme's active site is optimized for binding the lactone form of this degradation product.

MATERIALS AND METHODS

Overexpression, Purification, and Crystallization of ChiB from S. marcescens—Wild type chitinase B and the D142N mutant were overexpressed in *Escherichia coli* and purified as described elsewhere (27). The pure protein of wild type and D142N was lyophilized, dissolved to 1.0 mg/ml in 25 mM Tris buffer, pH 8, dialyzed overnight in the same buffer, and concentrated to 10 mg/ml before it was used in hanging drop vapor diffusion crystallization experiments. Crystals for wild type appeared within 3 days in 100 mM HEPES, pH 7, 10% glycerol, and 1.5 M ammonium sulfate. Crystals for the D142N mutant appeared within 3 days in 100 mM HEPES, pH 7, 15% glycerol and 1.3 M ammonium sulfate. Wild type and D142N crystals were soaked with 100-fold molar excess of HM508 for 1 month and 3 h, respectively, before being frozen in a nitrogen stream. Data were collected at beamline ID14 at the European Synchrotron Radiation Facility in Grenoble, France.

Further mutants of ChiB were produced by site-directed mutagenesis using the Stratagene (La Jolla, CA) QuikChange kit, as described previously (13, 17). Mutants were overexpressed and purified as described above.

Structure Determination—The data were processed using DENZO and scaled using SCALEPACK from the HKL suite (28). The previously published structure of the wild type enzyme in complex with allosami-

din (13) was used as template for an initial rigid body refinement. Both structures were refined in crystallography and NMR systems software (29), which included initial simulated annealing combined with iterative model building in O (30). The starting structure and molecular topology for HM508 were created using the PRODRG server (31). Two forms of the inhibitor were refined. For the D142N-HM508 data set, the full ligand was observed in the unbiased $|F_o| - |F_c|,\phi_{calc}$ density (Fig. 4) and included in the refinement. For the WT-HM508 data set, the unbiased $|F_o| - |F_c|,\phi_{calc}$ density in the active site and ESI-MS data (see below) showed a product of hydrolysis of HM508, *viz.* chitobionolactone. Refinement statistics are shown in Table I.

The crystals used for this study have two monomers in the asymmetric unit (named the A and B monomers) related by a 2-fold non-crystallographic axis (32). As with previous complexes, comparison of the monomers did not reveal significant conformational changes or differences in the binding site. The monomer best defined by the electron density maps was used for further analyses (the B monomer for the ChiB-HM508 complex and monomer A for the ChiB-D142N-HM508 complex).

Inhibition Studies—Before being used in enzyme assays, the lyophilized inhibitor was dissolved in doubly distilled water to yield a working solution of 1 mM. Chitinase activity was measured using 4-methylumbelliferyl-β-D-*N*,*N*′-diacetylchitobioside (Sigma) as a substrate. It has previously been shown that this assay permits accurate determination of kinetic parameters despite the fact that substrate inhibition necessitates the use of a relatively narrow range of (low) substrate concentrations (27). At first, inhibitor affinity was estimated by determination of IC_{50} values at 20 μM substrate concentration. Subsequently, K_i values were approximated by determining kinetic parameters (K_m, k_{cat}) in the presence of inhibitor at a concentration close to the IC_{50}. Calculation of kinetic and inhibitory parameters was performed using the curve fit option in the Enzyme Kinetics!Pro software package (ChemSW, Fairfield, CA).

Reaction mixtures for measurement of kinetic parameters contained 1.15 nM WT, 26 nM W220A, 10 nM D142N, or 16 nM M212A substrate at a concentration ranging from 5–20 μM (WT), 30–120 μM (W220A), 2.5–10 μM (D142N and M212A), and 0.1 mg/ml BSA in 50 mM citrate-phosphate buffer, pH 6.3. HM508 concentrations used were 100 μM (WT), 125 μM (W220A), 1 μM (D142N), and 1 μM (M212A). The reaction mixtures were incubated at 37 °C, and 50-μl samples were taken after 0, 2.5, 5, and 7.5 min and transferred immediately to 1.95 ml of 0.2 M Na_2CO_3 to stop the reactions. The amount of liberated 4-methylumbelliferyl was measured by fluorometry. Product formation was linear over time for all ChiB variants at all substrate concentrations.

Analysis of HM508 Degradation—To investigate degradation of HM508, wild type ChiB, ChiB-M212A, ChiB-D142N, and ChiB-W220A were incubated for 17 days at room temperature with and without HM508 under normal assay conditions without substrate. To accelerate the rate of degradation, the enzymes were used at a concentration higher than that for the published standard assay. The reaction mixtures contained 3.6 nM WT, 19 nM M212A, 57 nM D142N, or 98 nM W220A and 0.1 mg/ml BSA, in 50 mM citrate-phosphate buffer, pH 6.3. HM508 concentrations used were 75 μM (WT), 2 μM (M212A), 5 μM (D142N), and 200 μM (W220A). After 10 min and 1, 3, 9, 13, and 17 days of incubation, 45-μl samples were removed from these enzyme-inhibitor mixtures and from parallel control mixtures (enzyme without inhibitor) for determination of enzyme activity. Activities were determined by the addition of 5 μl of substrate (final concentration 20 μM) and by using standard conditions (T = 37 °C; pH = 6.3; incubation time = 10 min). All measurements were performed in duplicate. Activities in the enzyme-inhibitor mixtures are expressed as a percentage of the activity in the corresponding control sample (no inhibitor). The control reactions did not show any significant loss of activity during the incubation period.

ESI-MS was used to analyze degradation products of HM508 in the absence and presence of ChiB. 1 μM ChiB (wild-type or the D142N mutant) was incubated with 100 μM HM508 in 50 mM ammonium acetate buffer, pH 6 (the specific activity of ChiB in this buffer is similar to the specific activity in the citrate-phosphate buffer used in standard activity assays). We used high concentrations of enzyme and inhibitor to mimic the conditions during crystallization and soaking and to abolish the need for the addition of BSA as an enzyme stabilizer (BSA gave a dramatic increase in background noise in subsequent analyses). Samples were analyzed by ESI-MS at the start of the incubation and at various time points up to 30 days later.

ESI-MS analysis was conducted using a Micromass Quattro LC triple quadrupole instrument. The sample was introduced directly into the source using a syringe pump at a flow rate of 10 μl/min. Mass spectra were obtained in positive mode, with cone voltage at 30 V, capillary voltage at 3 kV, and multiplier voltage at 650 V. The desolvation and source block temperatures used were 160 and 80 °C, respectively. The mass scan range was 50–650 *m/z*.

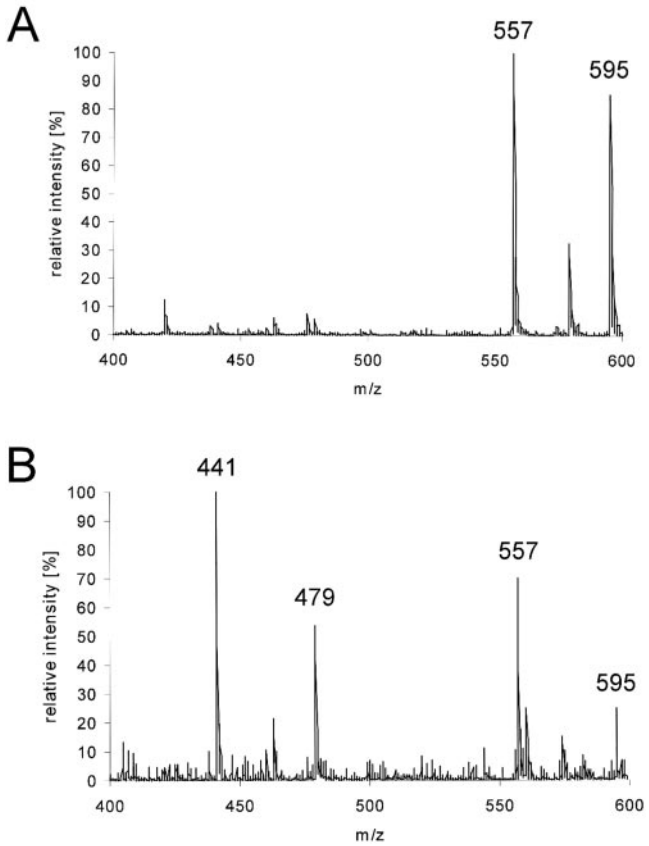

FIG. 2. **ESI-MS spectra of HM508 incubated with and without ChiB for 30 days.** *A*, HM508. *B*, HM508 plus wild type ChiB.

RESULTS

Inhibitor Stability—Initial crystallographic soaking studies of wild-type ChiB with HM508 suggested that the inhibitor was degraded. Therefore, we studied the possible degradation of HM508 by ChiB and a less active variant of ChiB (D142N) (13, 17) using relatively high concentrations of enzyme and inhibitor (thus mimicking to some extent the conditions during the crystal-soaking experiments). ESI-MS analyses of mixtures of ChiB and HM508 showed that a 557 peak corresponding to the intact inhibitor (557 for HM508 + H^+) and the K^+ adduct peak (595 for HM508 + K^+) disappeared over time, whereas a new set of peaks (441 for M + H and 479 for M + K^+) appeared (Fig. 2). As explained below, a hydrolytic reaction that would generate a compound with mass 440 would be the generation of a chitobionolactone (Fig. 1) in equilibrium with its hydroxy acid. The equilibrium between these compounds is expected to lie far toward the hydroxy acid at neutral pH (33). The degradation of the inhibitor was a slow process; after 17 days ~50% of the inhibitor had been degraded by the enzyme (Fig. 3). Conversion of HM508 to a compound with a molecular mass of 440 was not observed in the absence of enzyme (Fig. 2) nor in the presence of the less active D142N mutant of ChiB (not shown).

To explore the significance of the enzymatic HM508 degradation in our standard enzyme inhibition assays, ChiB, ChiB-M212A, ChiB-W220A, and ChiB-D142N were incubated for 17 days with and without HM508 under normal assay conditions with no substrate. Fig. 3 shows that the ChiB-D142N HM508 mixture was the only one with stable enzyme activity throughout the incubation period. For the remaining enzyme-inhibitor mixtures, activities gradually increased until they reached lev-

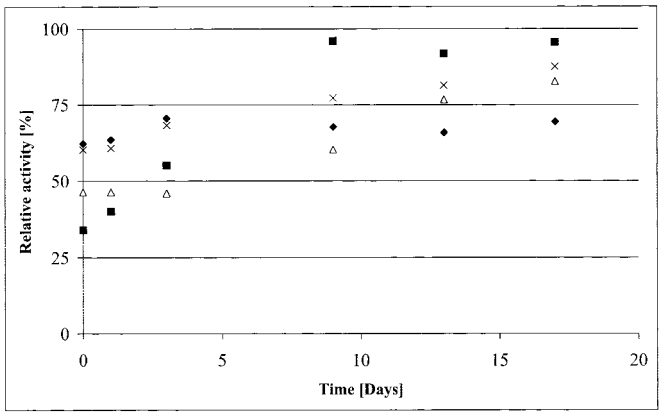

FIG. 3. **Effect of HM508 degradation on enzyme inhibition.** Enzyme activities are expressed relative to the activity in the samples without inhibitor; ChiB wild type (*triangles*), ChiB-M212A (*squares*), ChiB-D142N (*diamonds*), and ChiB-W220A (*crosses*).

els close to what was observed in the corresponding samples without HM508. These results confirm that degradation of the inhibitor is a slow process. Because degradation of the inhibitor occurs on a significantly longer time scale (days) than experiments for determination of kinetic parameters (minutes), the K_i values determined in this study apply to intact HM508.

Structural Analysis—Because of the degradation of HM508 in the wild type enzyme, the interaction of HM508 with ChiB was analyzed by solving the structure of HM508 in complex with the less active ChiB mutant (D142N) that did not show degradation of the inhibitor within the time scale of our experiments. In addition, we solved the structure of ChiB using a crystal that had been soaked with HM508 for several months to determine the structure of the degradation product. The ChiB-HM508 and ChiB-D142N-HM508 complexes were refined to 1.90 and 1.80 Å, respectively, with *R*-factors converging at R (R_{free}) = 0.209 (0.245) and 0.205 (0.255), respectively. Statistics of the refinement and the final models are shown in Table I. Both structures showed well defined unbiased $|F_o| - |F_c|,\phi_{calc}$ density in the −1 and −2 subsites that corresponded to the sugar moieties of the inhibitor (Fig. 4). In addition, the ChiB-D142N-HM508 maps showed density for the HM508 phenylcarbamate moiety, which interacts with the +1 and +2 subsites of the enzyme (Trp-97 and Trp-220; Fig. 4). In the D142N-HM508 structure, the −1 sugar lies toward the $^{1,4}B$ conformation, close to the conformation seen for the −1 sugar in a complex between an inactive mutant of ChiB (E144Q) and $GlcNAc_5$ (13) (Fig. 4).

In general, the active site architecture and the interactions between the disaccharide moiety and the enzyme are similar to those observed in the E144Q-$GlcNAc_5$ complex (13), as shown in Fig. 4 and Table II. One of two major differences concerns residue 142, which, in the E144Q-$GlcNAc_5$ complex and in most other ChiB-ligand complexes, hydrogen bonds to Glu-144 (13, 24). This hydrogen bond does not exist in the D142N-HM508 complex because the side chain of Glu-144 is in a different position (rotated 14° around χ_1, 32° around χ_2, and 86° around χ_3 compared with E144Q-$GlcNAc_5$) to hydrogen bond the N1 of the HM508 oxime (Fig. 4; Table II). A second difference concerns the position of the glycosidic oxygen in the E144Q-$GlcNAc_5$ structure and the equivalent N1 nitrogen of the HM508 oxime (shift of 1.1 Å). The electron density and the planar conformational restraints for the sp^2-hybridized C1 carbon place the oxime N1 0.9 Å closer to the conserved Met-212 than the equivalent glycosidic oxygen in the E144Q-$GlcNAc_5$ structure (Table II; Fig. 4). Although this does not directly generate a steric clash (distance between N1 and Met-212-Sδ is 3.7 Å compared with 4.6 Å for the equivalent distance in the E144Q-$GlcNAc_5$ complex), it does appear to distort the linker between the −1 sugar and the phenyl ring in HM508 from planarity (by as much as 27° over the oxime bond).

TABLE I
Refinement and structure quality statistics of WT-HM508 and D142N-HM508

Values in parenthesis are in the outer resolution shell. Crystals were of space group $P2_12_12_1$. No resolution or $I/\sigma I$ cutoffs were applied to the data used for the refinement. R.m.s.d. is root mean square deviation.

	WT-HM508	D142N-HM508
Unit cell (Å)		
a	55.34	55.52
b	103.48	104.17
c	186.02	185.99
Resolution (Å)	30–1.90 (1.97–1.90)	25–1.80 (1.86–1.80)
Observed reflections	321,320 (20,722)	347,374 (15,937)
Unique reflections	84,877 (7748)	97,967 (7746)
Redundancy	3.8 (2.7)	3.5 (2.1)
Mean $I/\sigma I$	9.3 (3.2)	25.9 (2.7)
Completeness (%)	99.0 (91.7)	97.1 (77.8)
R_{merge}	0.058 (0.37)	0.052 (0.30)
R_{cryst}	0.209	0.208
R_{free}	0.245	0.255
R_{free} reflections	1230	983
Protein atoms	7726	7816
Water molecules	756	892
Glycerol molecules	9	26
SO_4 molecules	7	7
Inhibitor molecules	2	2
R.m.s.d. from ideal geometry		
Bonds (Å)	0.014	0.010
Angles (°)	1.58	1.48
⟨B⟩ (Å^2) protein	29.8	32.2
⟨B⟩ (Å^2) HM508	24.8	28.2

The phenylcarbamate group hydrogen bonds with Asp-215-Oδ2 through the Nγ nitrogen and with Tyr-145-Oη through the Oβ oxygen (Figs. 1 and 4; Table II). The hydrophobic phenyl ring is located close to Trp-97 and Trp-220 that line the +1 and +2 subsites of ChiB. These two aromatic residues are shifted toward the ligand (up to 0.5 Å compared with the apo-D142N structure) (34). A similar, but larger displacement (shifts up to 1 Å) has previously been observed upon substrate binding to E144Q (13). Additionally, main chain movements of the loops covering the active site indicate a closure of the roof of the active site tunnel, equivalent to what was observed in the E144Q-$GlcNAc_5$ structure (13). The phenyl group does not form the triple sandwich with Trp-97 and Trp-220, as was observed in the E144Q-$GlcNAc_5$ structure for the +1/+2 sugars; rather, it interacts with these tryptophans in an orthogonal orientation. A similar interaction has been observed for the phenylalanine side chain in the cyclic pentapeptide inhibitor argifin (24).

In contrast to the D142N-HM508 complex, the WT-HM508 complex only shows a disaccharide bound to the −2 and −1 subsites. The unbiased $|F_o| - |F_c|,\phi_{calc}$ map for the ligand is well defined (Fig. 4), and, together with the high resolution (1.9 Å) data, suggests that it is not HM508 but rather a degradation product that occupies the binding site. The conformation of the sugar bound to the −2 subsite is essentially identical to that of the corresponding sugar in the D142N-HM508 structure (Fig. 4). However, unlike the D142N-HM508 structure, the −1 sugar is near the ^4E conformation, which is more similar to the expected transition state conformation. The density shows that the C1 carbon is sp^2-hybridized and makes three bonds, two within the pyranose ring and one to an extra hetero-atom attached to the ring. Together with chemical considerations (discussed below) and the results of the ESI-MS analyses of HM508 degradation, this suggests that the compound bound to

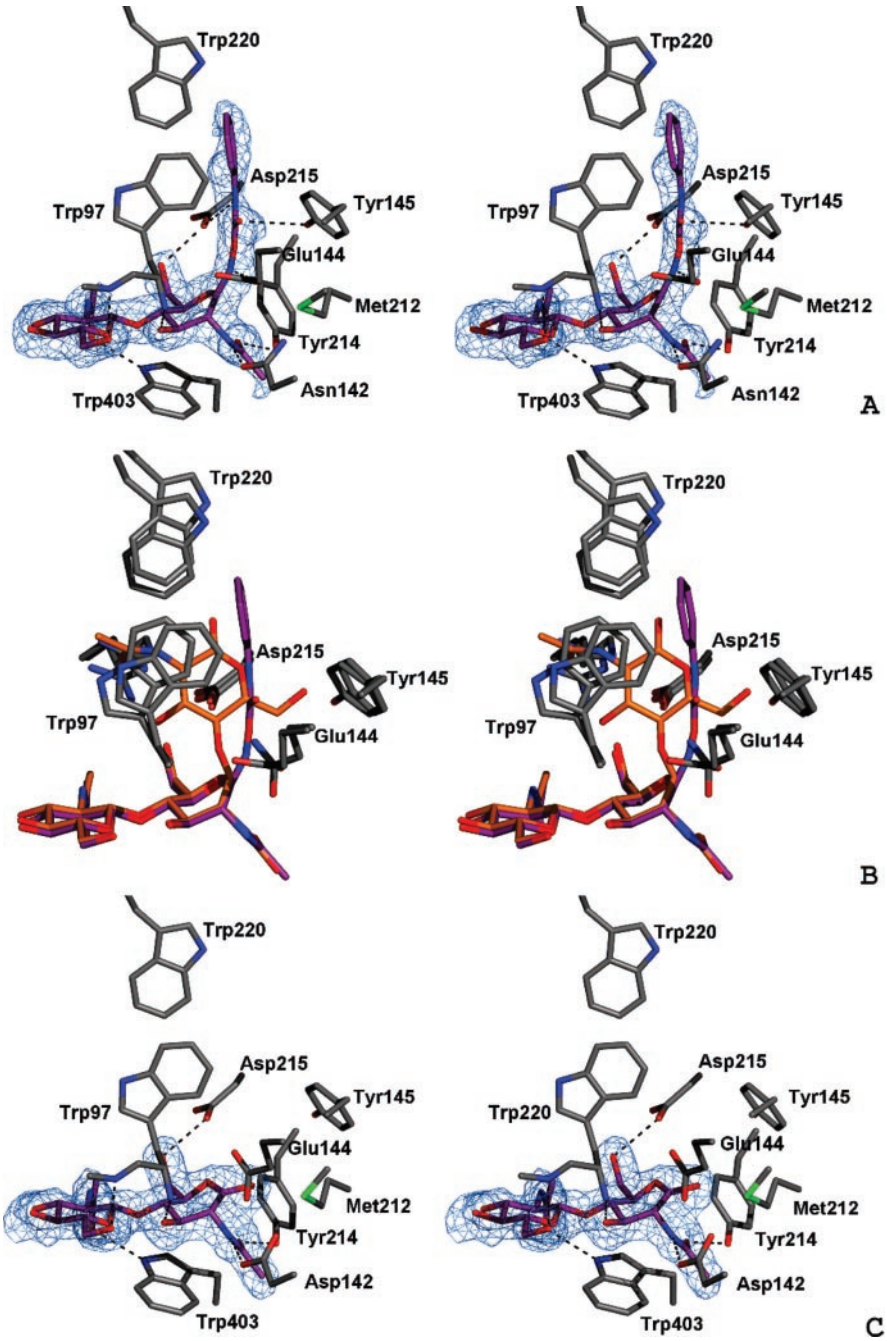

FIG. 4. **Structure of HM508 bound to the active site of ChiB and ChiB-D142N.** *A*, HM508 bound to the −1, −2, and +1/+2 subsites of ChiB-D142N. Protein side chains are drawn as *sticks*. HM508 is also shown with *purple stick* carbons. The unbiased $|F_o| - |F_c|,\phi_{calc}$ electron density contoured at 2.25 σ is also shown. Hydrogen bonds are represented by *black dashed lines*. *B*, comparison of the ChiB-D142N-HM508 complex with the published ChiB-E144Q-$GlcNAc_5$ structure (PDB code 1E6N) (13). Colors are as in *panel A*, with the −2 to 1 sugars of the $GlcNAc_5$ molecule shown with *orange carbons*. *C*, structure of the wild type ChiB-HM508 complex revealing a degradation product, the chitobiono-δ-lactone bound to the −1 and −2 subsites. The chitobiono-δ-lactone is shown as sticks with purple carbons. The unbiased $|F_o| - |F_c|,\phi_{calc}$ electron density map is also shown, contoured at 2.25 σ. Hydrogen bonds are shown as *black dashed lines*.

the active site is a chitobiono-δ-lactone (Fig. 1). The lactone oxygen is positioned even closer to Met-212-Sδ (distance = 2.7 Å; Fig. 4 and Table II) than the equivalent oxime nitrogen in the D142N-HM508 structure (distance = 3.7 Å). This causes Met-212 to rotate away from the lactone oxygen (149° around χ_2). The lactone oxygen and the catalytic acid Glu-144 are positioned such that no hydrogen bond with reasonable geometry can be formed.

Enzymology and Site-directed Mutagenesis—Table III shows kinetic constants and K_i values for ChiB, the D142N mutant, and two other mutants of ChiB (M212A and W220A), which were constructed and analyzed because these residues make key interactions with HM508. HM508 showed competitive inhibition in all cases. The K_i of wild type ChiB for HM508 was 45 μM. The D142N mutant displayed a 26-fold decrease in the K_i for HM508, together with a 59-fold reduced k_{cat} and a 7-fold reduced K_m (Table III). Thus, the D142N mutant binds HM508 significantly stronger than the wild type enzyme. The W220A mutant was studied to assess the possible contribution of stacking interactions in the +1/+2 subsites to HM508 binding. As expected, the W220A mutation increased K_m and K_i (3.5- and 5.4-fold, respectively), indicating that Trp-220 contributes to inhibitor (and substrate) binding (Table III). It had previously been shown that the same mutation does not affect the K_i for allosamidin, which only binds the −3 to −1 subsites (24).

The M212A mutant was constructed to evaluate the role of the observed close contacts between the Met-212 side chain (and the Sδ atom in particular) and the ligands. Previous studies have shown that Met-212 may play an important role in the binding of the distorted sugar to the −1 subsites (13). Mutation of Met-212 led to a 2.6-fold increase in K_m and an 8-fold decrease in k_{cat} (Table III). As expected, the M212A mutation (which removes the steric clash with the oxime; Fig. 4) yielded a reduction in the K_i (90-fold) for HM508, showing that the mutant binds HM508 stronger than the wild type enzyme.

TABLE II

Interactions observed in the −2, −1 and +1 subsites in the E144Q-GlcNAc$_5$, D142N-HM508, and WT-HM508 structures

Hydrogen bond donor-acceptor distances (D-A column) were calculated with WHAT IF (43), along with the geometrical quality of the hydrogen bonds (HB2 column), using the HB2 algorithm (44). The HB2 values range from 0 (no hydrogen bond) to 1 (optimal hydrogen bond). Weak hydrogen bonds (HB2 < 0.3) are not listed.

	D142N-HM508			E144Q-NAG5			WT-δ-lactone		
Subsite	H-bond	D-A	HB2	H-bond	D-A	HB2	H-bond	D-A	HB2
−2	Tyr-9 N-O6	3	0.79	Tyr-98 N-O6	3.1	0.88	Tyr-98N-O6	3	0.79
−2	Trp-403 Nε1-O7	2.9	0.66	Trp-403 Nε1-O7	3	0.66	Trp-403 Nε1-O7	2.9	0.70
−2	Gln-407 Nε2-O7	3.2	0.51	Gln-407 Nε2-O7	3.5	0.43	Gln-407 Nε2-O7	3.4	0.48
−1	Glu-144 Oε2-N1	2.8	0.59	Glu-144 Oε2-O4	3	0.90			
−1	Trp-97 N-O3	3	0.87	Trp-97 N-O3	3.1	0.90	Trp-97 N-O3	3.2	0.89
−1	Tyr-214 Oη-O7	2.6	0.78	Tyr-214 Oη-O7	2.6	0.75	Tyr-214 Oη-O7	2.6	0.77
−1	Asp-215 Oδ2-O6	2.7	0.89	Asp-215 Oδ2-O6	2.7	0.76	Asp-215 Oδ2-O6	2.8	0.95
−1	Asp-142 Oδ1-N2	2.8	0.80	Asp-142 Oδ1-N2	2.9	0.74	Asn-142 Oδ2-N2	2.8	0.90
+1	Tyr-145 Oη-O$_2$	3.3	0.51	Tyr-145 Oη-O6	2.7	0.59			

DISCUSSION

The designed chitinase inhibitor HM508 inhibits wild type ChiB with a K_i of 45 μM, which is in the same range as the K_i for natural product chitinase inhibitors such as argifin (4, 24) and psammaplin (35). The structural basis for this inhibition is defined by the 1.8-Å crystal structure of the D142N-HM508 complex. With respect to subsites −2 and −1, binding of HM508 resembles binding of the natural substrate as seen in the E144Q-GlcNAc$_5$ complex (13) (Fig. 4). Despite the sp^2 configuration of the C1 carbon, the −1 sugar is forced toward a ^{1,4}B conformation due to the steric clashes between Met-212 and the phenylcarbamate moiety in the +1/+2 subsite (Fig. 4). The increase in HM508 affinity observed for the M212A mutant confirms that the N1 atom of the inhibitor (which occupies a different position than the equivalent glycosidic oxygen) interacts unfavorably with Met-212. Met-212 is conserved in family 18 chitinases and contributes to the formation of a hydrophobic pocket for the oxazolinium ion methyl group (Figs. 1 and 4) (11–13, 22). It is possible that Met-212 could limit the affinity that might be achieved by further structure-based development of HM508-like inhibitors.

The phenylcarbamate moiety of HM508 is positioned between the tryptophans that define the +1/+2 subsites (Trp-220 and Trp-97) but is not stacked as a triple sandwich as is the case for the +1/+2 sugars in the E144Q-GlcNAc$_5$ structure (Fig. 4). The movement of Trp-220 and Trp-97 upon ligand binding was less evident in the D142N-HM508 structure than in the E144Q-E144Q-GlcNAc$_5$ structure (Fig. 4). The loss of inhibitory effect upon HM508 degradation (Fig. 3), the decreased inhibitor affinity of the W220A mutant (Table III), and the fact that chitobiose binds ChiB with low affinity (27) all show that the phenylcarbamate group is a key determinant of HM508 affinity. A possible strategy toward increasing inhibitor affinity would be to replace the phenyl group with a larger aromatic moiety.

The D142N mutant showed increased affinity for the substrate and displayed further increased affinity for HM508 (Table III). The structures do not provide an explanation for this increase in affinity, indicating that it could be due to the change in active site electrostatics that results from the mutation. The binding of a neutral inhibitor such as HM508 is likely to have unfavorable electrostatic effects, because two acidic residues (Asp-142 and Glu-144) become desolvated. This effect is reduced in the D142N mutant, which may explain the higher affinity for HM508. Degradation of HM508 by wild type ChiB occurs on a significantly longer time scale than the K_i measurements; thus, the higher affinity of D142N for HM508 is not simply due to the fact that the mutant does not degrade the inhibitor.

The observed degradation of HM508 prompted us to solve the structure of ChiB wild type soaked with the inhibitor over a longer period of time (several months). Surprisingly, the crystal structure revealed a chitobiono-δ-lactone bound to the −2 and −1 subsites, whereas ESI-MS analysis of degraded HM508 in solution only showed the hydroxy acid form of the lactone. δ-Lactones have been proposed to act like transition state analogues for glycoside hydrolases, mimicking the oxocarbenium ion that has a ^4E conformation (33, 36, 37). However, because of the instability of δ-lactones in solution, their usefulness as inhibitors has been limited (38). Secemski *et al.* (33) showed that the equilibrium for a tetra-*N*-chitotetraose δ-lactone is shifted toward 100% hydroxy acid at pH 4.7. This study also showed that at pH 2.1–2.3, the equilibrium was driven toward 14% of the δ-lactone form. Ford *et al.* used a low pH (2.6) when they demonstrated binding of the δ-lactone of chitotetraose to lysozyme (36). The fact that we observed the chitobiono-δ-lactone in the active site of ChiB at a pH as high as 8 (the pH of the crystallization mother liquor) suggests that the enzyme favors the δ-lactone over the hydroxy acid form. This is in agreement with the notion that the enzyme is optimized for binding sugars in a conformation that is close to the proposed ^4E transition state (Fig. 1) (12, 13, 37). Although the δ-lactone interacts unfavorably with Met-212, the hydroxy acid form would create more unfavorable interactions, not only in the form of steric clashes (*e.g.* with Asp-215 and Glu-144; Fig. 4) due to the opened pyranose ring but also potential electrostatic repulsion because the ChiB active site is negatively charged (Asp-140, Asp-142, Glu-144, and Asp-215; Fig. 4).

Despite the crystallographically observed binding of a degradation product of HM508 (the chitobiono-δ-lactone) to the wild type ChiB active site, degraded HM508 did not show detectable inhibition of ChiB. This is probably due to the low concentration of the δ-lactone form in solution and to the reduction in affinity caused by the close contact between the lactone oxygen and Met-212 (Fig. 4 and Table II; note that this oxygen is absent in the oxocarbenium transition state, where it is a hydrogen (Fig. 1). The fact that the chitobiono-δ-lactone is crystallographically observed in the active site does not necessarily mean that its affinity for ChiB is sufficiently high to yield detectable inhibition in solution. It is known from other studies with ChiB that low affinity compounds may bind in a specific fashion to the active site (39).[2]

TABLE III

Kinetic parameters and inhibition constants for ChiB variants

Enzyme	K_m	k_{cat}	K_i HM508
	μM	s^{-1}	μM
WT	24 ± 2	10 ± 0.5	45 ± 2
W220A	84 ± 4	0.50 ± 0.01	243 ± 11
D142N	3.5 ± 2.2	0.17 ± 0.07	1.7 ± 0.4
M212A	6.3 ± 1.0	1.2 ± 0.2	0.50 ± 0.05

[2] D. R. Houston, M. J. R. Stark, I. Eggleston, V. G. H. Eijsink, and D. M. F. van Aalten, manuscript in preparation.

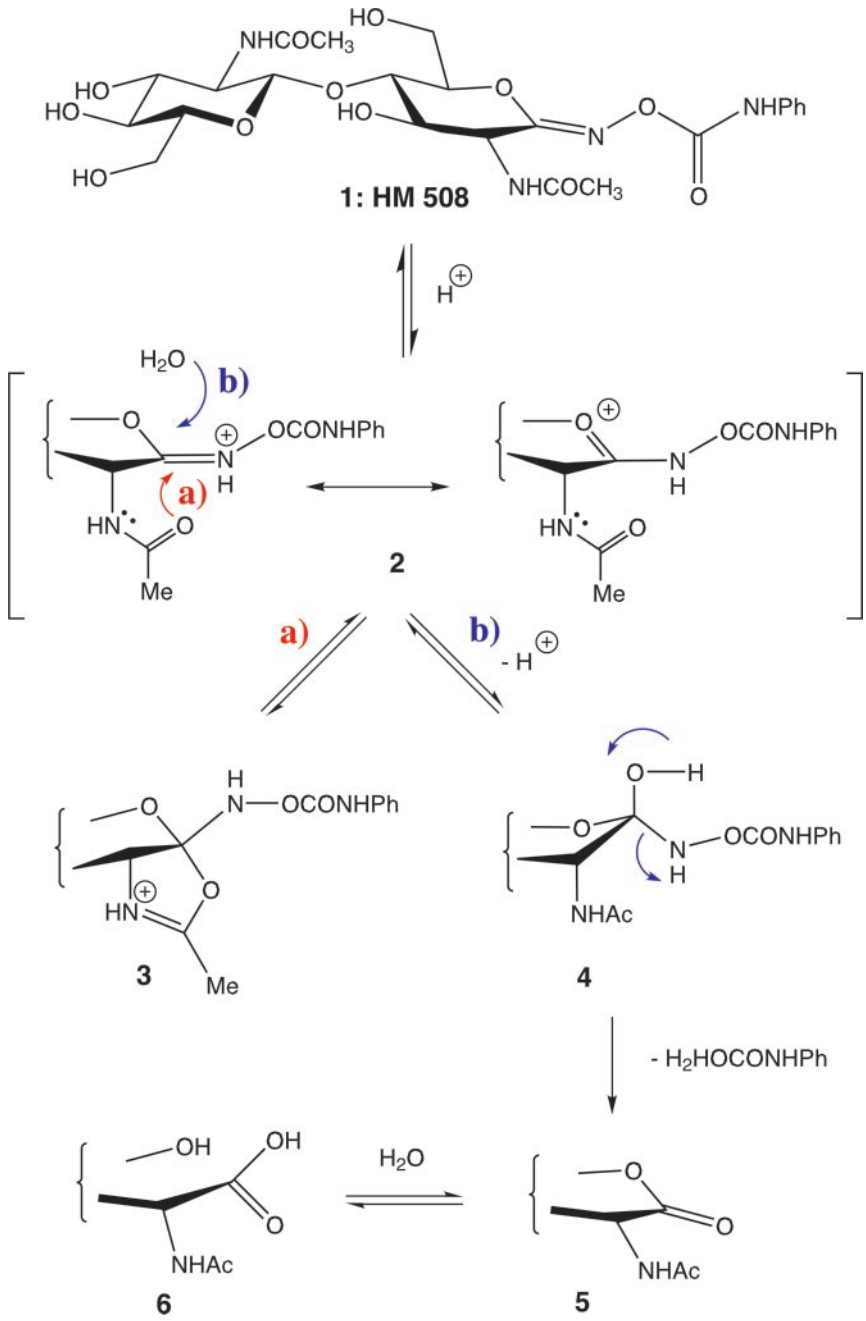

FIG. 5. **Proposed reaction scheme for HM508 degradation by ChiB.**

The data presented here show that HM508 is enzymatically degraded to chitobiono-1,5-lactone. The mechanism of the enzyme catalyzed hydrolysis of the *O*-carbamoyl hydroximolactone HM508 is shown in Fig. 5. Protonation of the oxime N1 by Glu144 leads to a resonance stabilized intermediate that possesses partial oxycarbenium cation character (labeled *2* in Fig. 5). *A priori*, the carbonyl oxygen can attack this cation to give the oxazolinium cation *3* (pathway labeled *a* in Fig. 5). Steric hindrance of the anomeric carbon precludes an S_N2 type substitution at C1 by water. However, opening of the oxazolinium cation by an S_N1 type process leads back to intermediate *2*, and attack of water will occur at this stage. The resulting 1-*N*-acylaminopyranose decays in an acid catalyzed reaction to give the lactone *5* and the known *O*-((phenylamino)carbonyl)-hydroxylamine (41, 42). Interestingly, the D142N mutant does not show the ability to hydrolyze HM508. Structurally, there is a key difference that can account for the inability of the D142N mutant to process HM508. In the D142N-HM508 complex, Glu-144 has lost its interaction with Asn-142 (Fig. 4), an interaction that is believed to lower the pK_a of Glu144, promoting proton transfer to the glycosidic oxygen (13), in this case the N1 of HM508.

The inhibition by HM508 and the structural analyses discussed above show that occupation of the +1/+2 subsites contributes in a decisive manner to inhibition. The degradation of the enzyme-bound HM508 evidences that this inhibitor makes use of the catalytic machinery of the enzyme. This is remarkable, as the sp^2 hybridization of the anomeric center marks HM508 as a transition state analogue rather than as a substrate analogue. The design and synthesis of inhibitors possessing a similar shape as HM508, with an optimized aromatic side chain and increased stability to the action of chitinases, should lead to stronger, useful inhibitors.

Acknowledgments—We thank Xiaohong Jia for technical assistance, Erlend Hvattum for help with the ESI-MS, and Yngve Stenstrøm for

helpful discussions. We thank the European Synchrotron Facility (Grenoble, France) for the time at beamline ID14.

REFERENCES

1. Henrissat, B. (1991) *Biochem. J.* **280,** 309–316
2. Henrissat, B., and Bairoch, A. (1993) *Biochem. J.* **293,** 781–788
3. Henrissat, B., and Bairoch, A. (1996) *Biochem. J.* **316,** 695–696
4. Arai, N., Shiomi, K., Yamaguchi, Y., Masuma, R., Iwai, Y., Turberg, A., Koelbl, H., and Omura, S. (2000) *Chem. Pharm. Bull.* **48,** 1442–1446
5. Cohen, E. (1993) *Arch. Insect Biochem. Physiol.* **22,** 245–261
6. Sakuda, S., Isogai, A., Matsumoto, S., and Suzuki, A. (1987) *J. Antibiot.* (*Tokyo*) **40,** 296–300
7. Izumida, H., Nishijima, M., Takadera, T., Nomoto, A. M., and Sano, H. (1996) *J. Antibiot* (*Tokyo*) **49,** 829–831
8. Vinetz, J. M., Valenzuela, J. G., Specht, C. A., Aravind, L., Langer, R. C., Ribeiro, J. M. C., and Kaslow, D. C. (2000) *J. Biol. Chem.* **275,** 10331–10341
9. Vinetz, J. M., Dave, S. K., Specht, C. A., Brameld, K. A., Xu, B., Hayward, R., and Fidock, D. A. (1999) *Proc. Natl. Acad. Sci. U. S. A.* **96,** 14061–14066
10. Tsai, Y.-L., Hayward, R. E., Langer, R. C., Fidock, D. A., and Vinetz, J. M. (2001) *Infect. Immun.* **69,** 4048–4054
11. Terwisscha van Scheltinga, A. C., Armand, S., Kalk, K. H., Isogai, A., Henrissat, B., and Dijkstra, B. W. (1995) *Biochemistry* **34,** 15619–15623
12. Tews, I., Terwisscha van Scheltinga, A. C., Perrakis, A., Wilson, K. S., and Dijkstra, B. W. (1997) *J. Am. Chem. Soc.* **119,** 7954–7959
13. van Aalten, D. M. F., Komander, D., Synstad, B., Gåseidnes, S., Peter, M. G., and Eijsink, V. G. H. (2001) *Proc. Natl. Acad. Sci. U. S. A.* **98,** 8979–8984
14. Bokma, E., Rozeboom, H. J., Sibbald, M., Dijkstra, B. W., and Beintema, J. J. (2002) *Eur. J. Biochem.* **269,** 893–901
15. Bortone, K., Monzingo, A. F., Ernst, S., and Robertus, J. D. (2002) *J. Mol. Biol.* **320,** 293–302
16. Watanabe, T., Kobori, K., Miyashita, K., Fujii, T., Sakai, H., Uchida, M., and Tanaka, H. (1993) *J. Biol. Chem.* **268,** 18567–18572
17. Synstad, B., Gaseidnes, S., Vriend, G., Nielsen, J. E., and Eijsink, V. G. H. (2000) in *Advances in Chitin Science* (Peter, M. G., Muzzarelli, R. A. A., and Domard, A., eds) Vol. 4, pp. 524–529, University of Potsdam, Potsdam, Germany
18. Sakuda, S., Isogai, A., Matsumoto, S., Suzuki, A., and Koseki, K. (1986) *Tetrahedron Lett.* **27,** 2475–2478
19. Sakuda, S. (1996) in *Chitin Enzymology* (Muzzarelli, R. A. A., ed) Vol. 2, pp. 203–212, Atec Edizioni, Ancona, Italy
20. Terwisscha van Scheltinga, A. C., Kalk, K. H., Beintema, J. J., and Dijkstra, B. W. (1994) *Structure* **2,** 1181–1189
21. Papanikolau, Y., Tavlas, G., Vorgias, C. E., and Petratos, K. (2003) *Acta Crystallogr. Sect. D Biol. Crystallogr.* **59,** 400–403
22. Rao, F. V., Houston, D. R., Boot, R. G., Aerts, J. M. F. G., Sakuda, S., and van Aalten, D. M. F. (2003) *J. Biol. Chem.* **278,** 20110–20116
23. Shiomi, K., Arai, N., Iwai, Y., Turberg, A., Koelbl, H., and Omura, S. (2000) *Tetrahedron Lett.* **41,** 2141–2143
24. Houston, D. R., Shiomi, K., Arai, N., Omura, S., Peter, M. G., Turberg, A., Synstad, B., Eijsink, V. G. H., and van Aalten, D. M. F. (2002) *Proc. Natl. Acad. Sci. U. S. A.* **99,** 9127–9132
25. Berecibar, A., Grandjean, C., and Siriwardena, A. (1999) *Chem. Rev.* **99,** 779–844
26. Beer, D., Maloisel, J. L., Rast, D. M., and Vasella, A. (1990) *Helv. Chim. Acta* **73,** 1918–1922
27. Brurberg, M. B., Nes, I. F., and Eijsink, V. G. H. (1996) *Microbiology* **142,** 1581–1589
28. Otwinowski, Z., and Minor, W. (1997) *Methods Enzymol.* **276,** 307–326
29. Brunger, A. T., Adams, P. D., Clore, G. M., Gros, P., Grosse-Kunstleve, R. W., Jiang, J.-S., Kuszewski, J., Nilges, M., Pannu, N. S., Read, R. J., Rice, L. M., Simonson, T., and Warren, G. L. (1998) *Acta Crystallogr. Sect. D Biol. Crystallogr.* **54,** 905–921
30. Jones, T. A., Zou, J. Y., Cowan, S. W., and Kjeldgaard, M. (1991) *Acta Crystallogr. Sect. A* **47,** 110–119
31. van Aalten, D. M. F., Bywater, R., Findlay, J. B. C., Hendlich, M., Hooft, R. W. W., and Vriend, G. (1996) *J. Comput. Aided Mol. Des.* **10,** 255–262
32. van Aalten, D. M. F., Synstad, B., Brurberg, M. B., Hough, E., Riise, B. W., Eijsink, V. G. H., and Wierenga, R. K. (2000) *Proc. Natl. Acad. Sci. U. S. A.* **97,** 5842–5847
33. Secemski, I. I., Lienhard, G. E., and Lehrer, S. S. (1972) *J. Biol. Chem.* **247,** 4740
34. Kolstad, G., Houston, D. R., Rao, F. V., Peter, M. G., Synstad, B., van Aalten, D. M. F., and Eijsink, V. G. H. (2003) *Biochim. Biophys. Acta*, in press
35. Tabudravu, J. N., Eijsink, V. G. H., Gooday, G. W., Jaspars, M., Komander, D., Legg, M., Synstad, B., and van Aalten, D. M. F. (2002) *Bioorg. Med. Chem.* **10,** 1123–1128
36. Ford, L. O., Johnson, L. N., Machin, P. A., Phillips, D. C., and Tjian, R. (1974) *J. Mol. Biol.* **88,** 349–371
37. Davies, G. J., Ducros, V. M. A., Varrot, A., and Zechel, D. L. (2003) *Biochem. Soc. Trans.* **31,** 523–527
38. Heightman, T. D., and Vasella, A. T. (1999) *Angew. Chem. Int. Edit. Engl.* **38,** 750–770
39. Houston, D. R., Eggleston, I., Synstad, B., Eijsink, V. G. H., and van Aalten, D. M. F. (2002) *Biochem. J.* **368,** 23–27
40. Brameld, K. A., and Goddard, W. A. (1998) *J. Am. Chem. Soc.* **120,** 3571–3580
41. Ketz, E. U., and Zinner, G. (1976) *Arch. Pharm.* **309,** 741–747
42. Rougny, A., and Daudon, M. (1976) *Bull. Soc. Chim. Fr.* **1,** 833–888
43. Vriend, G. (1990) *J. Mol. Graph.* **8,** 52–56
44. Hooft, R. W. W., Sander, C., and Vriend, G. (1996) *Proteins* **26,** 363–376